

Research Article

Novel Synthesis of Polyimide Foams with Aromatic and 1,6-Diaminohexane Imide Bonding

Dong-Sen Chen ¹, Chun-Hua Chen ¹, Wha-Tzong Whang,¹ and Chun-Wei Su²

¹Department of Materials Science & Engineering, National Yang Ming Chiao Tung University, 1001 Ta Hsueh Road, Hsinchu, Taiwan

²Material and Chemical Research Laboratories, Industrial Technology Research Institute, 195, Sec. 4, Chung Hsing Rd., Chutung, Hsinchu, Taiwan

Correspondence should be addressed to Chun-Hua Chen; chunhuachen@nycu.edu.tw

Received 29 March 2022; Revised 13 November 2022; Accepted 17 November 2022; Published 5 December 2022

Academic Editor: Gyorgy Szekely

Copyright © 2022 Dong-Sen Chen et al. This is an open access article distributed under the Creative Commons Attribution License, which permits unrestricted use, distribution, and reproduction in any medium, provided the original work is properly cited.

A novel type of polyimide foams (PIFs) with chemically inserted flexible aliphatic diamine (1,6-diaminohexane (HMDA)) segments was successfully synthesized and characterized in this research. The aliphatic HMDA segments were randomly incorporated in the long chain aromatic imide bonds. The obtained PIFs containing various HMDA contents (0 to 20 mol%) exhibited different morphologies such as lowered density and larger cell diameter (with higher HMDA content), and open cell ratio was increased as well. HMDA rendered flexibility to the copolymer leading to decreased rigidity. Compared to using 4,4'-oxydianiline (ODA) as the sole diamine source, incorporating low cost of HMDA would increase the PIF's flexibility and improve its processibility while making the production more cost effective. Within some range of compromised thermal and mechanical properties, this proposed method could be feasible for industrial applications.

1. Introduction

Aromatic polyimide (PI) owes its rigidity and thermal durability to its stiff aromatic backbone with imide rings, as reported in many papers in polymer related journals. Researches have actively endeavored to exploring various applications in areas such as membranes, coatings, foams, aerospace, and many more [1–6]. Such special chemical features are the reasons why the PI polymer has long been classified as high-performance polymer. Besides PI's many desirable properties, it can work with other chemical compounds for the productions of copolymers and various types of composited materials, while delivering its advantageous original properties to the new materials.

However, the chemical characteristic of the aromatic rings on the PI chain leads to high rigidity and strong inter-macromolecular interactions and consequently resulted in difficulties in processing. [7–12]. To surpass these difficulties, one plausible method is to insert function groups as

linkage to the aromatic chain that could render the polymer flexibility and/or to attach bulky function groups to the non-coplanar sides of the aromatic chain that may interfere with the aromatic stacking [13–15]. As reported by other researchers, the insertion of flexible aliphatic sequences in the rigid aromatic PI chain could lead to products possessing properties from both and could serve as a good strategy in designing new PI related copolymers that will meet various requirements [16–20].

However, in doing so, the mechanical and thermal durability could be affected due to change in the original molecular regularities of the original PI polymer. In the PI copolymers with added flexibility, Cristea et al. [17] studied semialiphatic 3,3',4,4'-benzophenonetetracarboxylic dianhydride (BTDA), 4,4'-diaminodiphenylmethane (DDM), and 1,6-diaminohexane (HMDA) to synthesize BTDA-based copolyimides with part of the DDM replaced by HMDA at different levels. They reported that above certain range of HMDA content, the PI copolymer behaved like elastomers.

McGrath et al. and Liaw et al. [21–23] reported a type of polyimide-polyorganosiloxane segmented copolymer exhibited improved processibility, toughness, flexibility, membrane performance, and adhesion, and by controlling the siloxane block length, the process could generate randomly segmented copolymers.

Nowak et al., Park et al., and Yang et al. [24–26] synthesized green polyamide thin-film composite membranes on a porous support on which plant-based genipin in the aqueous phase and priamine in the green organic solvent for forming composite thin-film membranes. Ikeda et al. [1] developed a technology that allows metallization (with copper ions) of polyimide films. These are only a few among many new arenas of R&D activities of various perspective on the basis of PI polymers.

In places where properties like light weight, rigidity, and thermal insulation were demanded, PI foams (PIFs) that possessed high mechanical strength, thermal dimensional stability, and flame retardancy were developed since the sixties [27]. Since then, the number of reports related to PIFs has been actively growing at an accelerated pace, especially in recent years [28–32]. Meanwhile, PIFs also have other applications, such as acoustic absorption, fire retardant, thermal durability, and electrical stability [33–35].

For increasing safety and energy efficiency demands, the need of foams with high mechanical strength, thermal stability, and light weight have been expanding, especially in the airplane and aerospace industries. PIFs were incorporated with reinforcement to obtain PI composites for enhancing the mechanical strength. Zhang et al. [36] composited PI which chopped carbon fibers to enhance the mechanic strength. Yan et al. [37] dispersed vermiculite in isocyanate to improve thermal properties of the flexible polyimide composite foams (as from dianhydride and isocyanate). Tian et al. [38] copolymerized polyimide with polyurethane and composited with silicon carbide and successfully enhanced the thermal durability. Zhou et al. produced high-performance electromagnetic interference (EMI) shielding material using polyimide-based PI composite foams assembled with polyimide bilayer coating. Later, the advanced polyimide bilayer PI coating was applied as protecting layer for EMI shielding [39].

Increasing crosslink density is yet another strategy in modifying PI copolymers. Meador et al. [40] used monomers with rigid segment and/or cross-linking agent for the polyimide main chains to increase the PIF's rigidity. Chu et al. [41] developed a PIF that by crosslinking with 2,4,6-triaminopyrimidine which has ultralow dielectric constant with improved mechanical properties. However, the increased melt viscosity resulted from added agents was a concern in the foaming process as reported by the authors.

Controlling the molecular weight by using end-capped oligomers is yet another strategy adopted by some researchers. Li et al. and Wang et al. [42, 43] used end-capped imide oligomers of dicarboxylic dianhydride, diamines, and reactive end-capping agent which were cross linked by evolved compounds. PIF with rigid closed cell, high thermal stability, and mechanical strength was obtained.

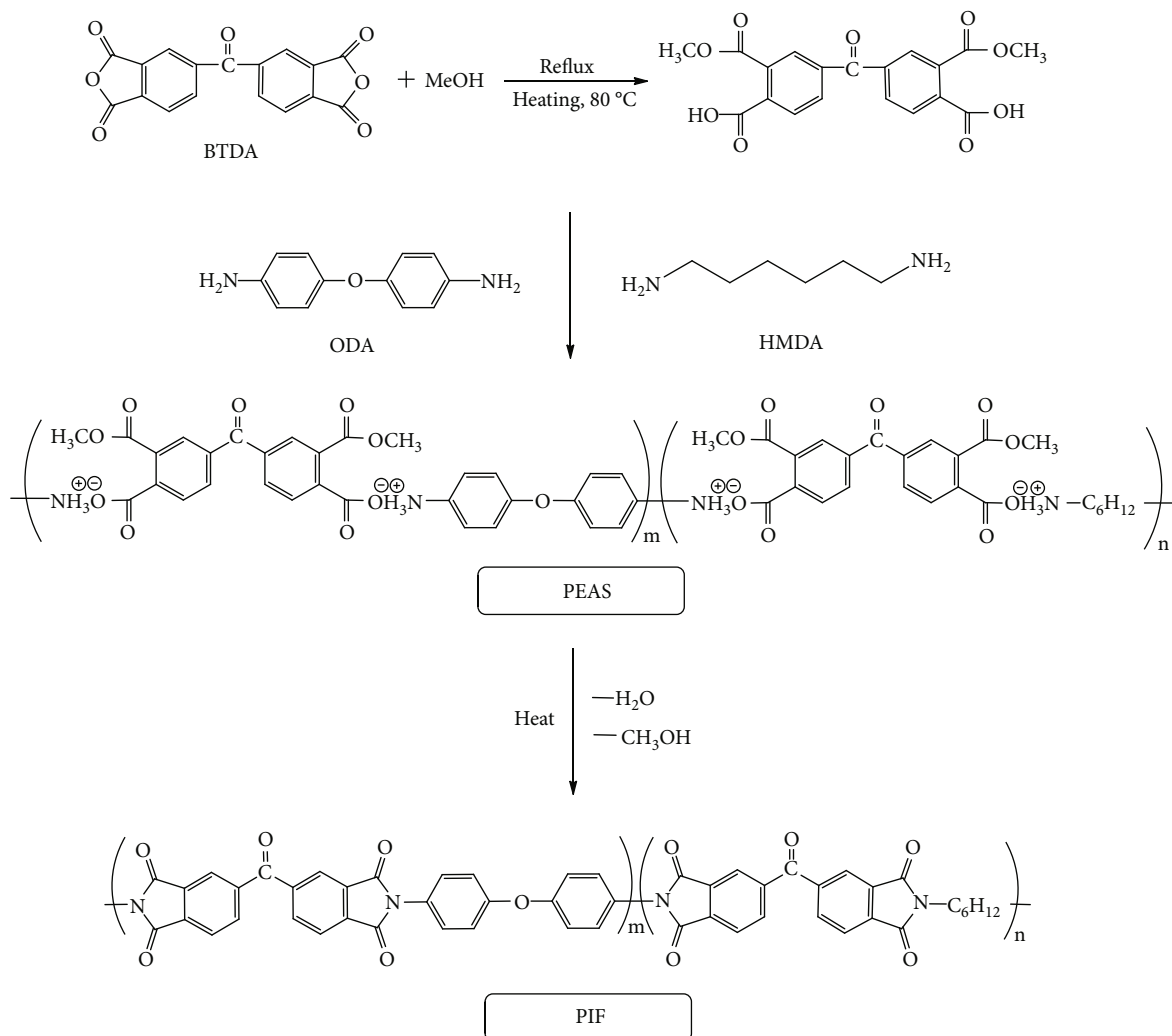
Chemically inserts other monomers to enhance rigidity have been performed by some researchers. Li et al. [44] synthesized PIFs contained benzimidazole units. They reported that the incorporation of 2-(4-aminophenyl)-5-aminobenzimidazole into the PI molecular chain significantly improved the thermal and mechanical properties.

Besides the above discussed various strategies, processibility is another concern that should not be overlooked. Copolymerization PI with another flexible segment would improve the PI copolymer's flexibility and therefore better processibility. Zhang et al. [45] studied the effect of adjusting the ratio of the flexible blocks (4,4'-diaminodiphenylsulfone (DDS)) in the range of 0 to 30 mol% which were linked into the rigid polymer ((2-(4-aminophenyl)-1H-benzimidazol-5-amine (APBIA) and 3,3',4,4'-biphenyltetracarboxylic dianhydride (BPDA)) to form a thermoplastic PIF. Liu et al. [46] modified PIFs by reacting with polyaryl polymethylene isocyanate for improved flexibility. Sun et al. [47] studied enhanced effects by refilling aromatic dianhydride on isocyanate-based PIFs.

Among many PIF related reports, polyester ammonium salt (PEAS) precursor was another favored process for PIFs fabrication. Li et al. [48–52] reported that several types of strategies in synthesizing PIFs still have room for improvement. However, the method of powder foaming using powdered form PEAS precursor in the fabrication, by manipulating the PEAS particle size, PIFs with different characteristics could be obtained. During the foaming process, generated methanol and water could act as blowing agents [50–53]. Yang et al. [] reported that the structure of PEAS precursor powders affects the melt viscosity during processing and, consequently, determined the cell structure and the product's physical properties. Ni et al. [] synthesized PIFs with PEAS precursor powders consisting different dianhydride structures as the derivatives. Besides that, the main feature of their preparation processing strategy is "microwave-assisted heating followed by post curing process".

The above-mentioned reports all have different merits in their own ways and are inspirational to researchers following their footsteps. Besides pursuing high quality, the industries must take other factors into considerations, such as processibilities, flexibilities, availabilities, and costs of raw materials. In this study, we intend to replace partially ODA by HMDA molecules into the commonly used BTDA/ODA PI polymer (for PI foaming). Hopefully the flexibility and processibility could be both increased without compromising too much the PI's original desirable properties. Cristea et al. [17] used HMDA to replace partially the BTDA/DDM in the PI copolymer, and increased flexibility was obtained. Varganici et al. [19] used various combination of BTDA with various aromatic, aliphatic (e.g. HMDA), or cycloaliphatic diamines to obtain flexible PI polymer. Their idea could be extended to the synthesis of PIFs in this study.

The concerns in this study are three folds: (1) broadening the PI applications in places where advantages are needed and, to some extent, compromising high PI quality are acceptable, but added flexibility function is also required; (2) providing the industries an option in fabricating foams possessing some of the PI properties and demonstrate how



SCHEME 1: Synthesis of PIFs with ODA partially replaced by HMDA.

the variables could be manipulated for specific requirement; (3) using readily available and inexpensive materials is always a good choice for the industries.

2. Experimental

2.1. Chemicals. 4,4'-Oxydianiline (ODA, reagent grade 98%) was purchased from Alfa Aesar Fine Chemicals & Metals (MA, USA), recrystallized from ethanol, and dried under nitrogen atmosphere before use. 1,6-Diaminohexane (HMDA; reagent grade, 95%) was purchased from Fluka Chemical (NY, USA). Methanol (HPLC grade, 99.9%) was purchased from Aencore Chemical (Surrey Hills, AU). BTDA (reagent grade 96%) was purchased from Sigma-Aldrich (MO, USA), recrystallized from acetic anhydride under nitrogen atmosphere, and vacuum dried before use. All other chemicals were used as received.

2.2. Synthesis. Polyimide foams (PIFs) with various compositions were synthesized according to a typical route with minor modification, in which powdered PEAS precursor was first prepared [41, 54–56]. Recrystallized BTDA

TABLE 1: Compositions of BTDA/ODA-HMDA based polyimide foams (PIF-mol% refers to mol% of HMDA in PIF).

PIF-mol%*	PIF-0	PIF-5	PIF-10	PIF-15	PIF-20	PIF-100
BTDA (mol)	0.06	0.06	0.06	0.06	0.06	0.06
ODA (mol)	0.06	0.057	0.054	0.051	0.048	0
HMDA (mol)	0	0.003	0.006	0.009	0.012	0.06

(32.33 g, 100 mmol) was first suspended in 100 mL anhydrous methanol and refluxed with continuous stirring for 2 h. A solution of 3,3',4,4'-benzophenone diacid dimethylester derivative in methanol was then obtained (Scheme 1).

ODA and HMDA at various molar ratios (Table 1) were added to the above diacid dimethylester methanol solution. After stirring at room temperature for 3 h in nitrogen, PEAS solution in methanol was obtained. Methanol was then removed by vacuum heating, and solid PEAS precursor BTDA/ODA-HMDA (Scheme 1) was obtained. The recovered solid PEAS precursor was ground and sieved to its powder form (100 mesh) for subsequent imidization foaming reactions.

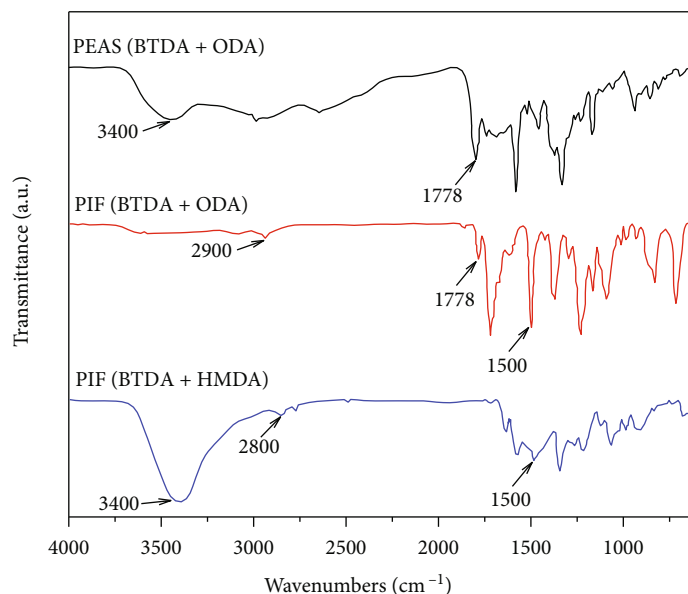


FIGURE 1: FTIR spectrum of PEAS (BTDA + ODA), PIF(BTDA + ODA) and PIF (BTDA + HMDA).

In order to fix the total carbonyl (C=O) to amine ($-\text{NH}_2$) molar ratio and to assure high molecular weight, the number of moles of added HMDA was controlled that the total molar amounts of diamine in ODA and HMDA was equal to the molar amounts of dianhydride (Table 1). Thus, the comparisons and characterizations in this study would be based on approximately the same number of imide bonding in the final PIFs of various designed HMDA content.

2.3. Foaming and Imidization. Weighed PEAS powder was spread evenly in a stainless-steel box (15 cm by 10 cm, 15 cm deep) and put in an oven. The oven temperature was raised to 150°C at a rate of 2.0°C/min. As shown in Scheme 1, condensation reaction between amide and methyl ester (in the long chain PEAS) proceeded with rising temperature. One molecule each of water and methanol was released per imide bonding formed (imidization of PEAS). The generated water (boiling point about 100°C) and methanol (boiling point about 65°C) vaporized at temperature far below 150°C. Vaporized water and methanol underwent volume expansion at temperature above their boiling point and served as foaming agent. The oven temperature was further raised to 300°C and hold for another 1.5 h for curing and imidization of possible unreacted amide and methyl ester.

2.4. Instrumental Analysis. FTIR spectroscopy in KBr pellets (Bio-Rad FTS-155, Bio-Rad Laboratories Inc., USA) was used to study the patterns of variations in absorption peaks pertaining to featuring function groups. Samples were ground with KBr to fine powders then pressed in to thin disc for scanning.

Thermal Gravimetric Analysis in nitrogen (TGA, TA Instrument TGA-2050, DE, USA) was used to compare the thermal durability of PIFs with various HMDA content. Differential scanning calorimetry (DSC, TA Instrument MDSC 2920, DE, USA) was used to compare the glass transition

temperature (T_g) of PIFs. Samples were ground to fine powders. Scanning electron microscope (SEM; Hitachi JSM-6300:S-550, Japan) was used to take pictures for analyzing and comparing cell sizes of PIFs. Small pieces of samples were coated with platinum spotter.

2.5. Physical Measurements. Physical measurement of the densities of the foam, open/closed cells were done according to ISO-845-2006 and ASTM-D6226, respectively. Rigidity of the PIFs with various HMDA content was compared using a universal tensile testing machine (Testometric M500-25AT, UK) according to ISO-604-2001. The stress at 10% compressed deformation was compared for various synthesized PIFs.

3. Results and Discussions

3.1. Reactions between BTDA and ODA or HMDA. As described in the experimental section, recrystallized BTDA was first refluxed in methanol for 2 hours during which the diacid anhydride ring was opened to form a methyl ester and a carboxylic acid function groups. Thus, formed intermediate was a diacid methylester derivative (step 1 in Scheme 1). The acid ($-\text{COOH}$) part will then be available for neutralization with $-\text{NH}_2$ (of ODA and/or HMDA) to produce PEAS (step 2 in Scheme 1). The PEAS precursor was then ground and sieved to obtain fine PEAS powders (ca. 100 mesh) for later foaming process. Fine powdered PEAS will facilitate a more evenly precursor distribution which is beneficial to subsequent imidization and foaming processes.

For PIF synthesized from BTDA/ODAD, both reactants were benzene ring based, and these materials have long history of industrial applications [1–6]. However, when we wish to insert an aliphatic segment between bulky aromatic groups that are mainly constituted of benzene rings, it is

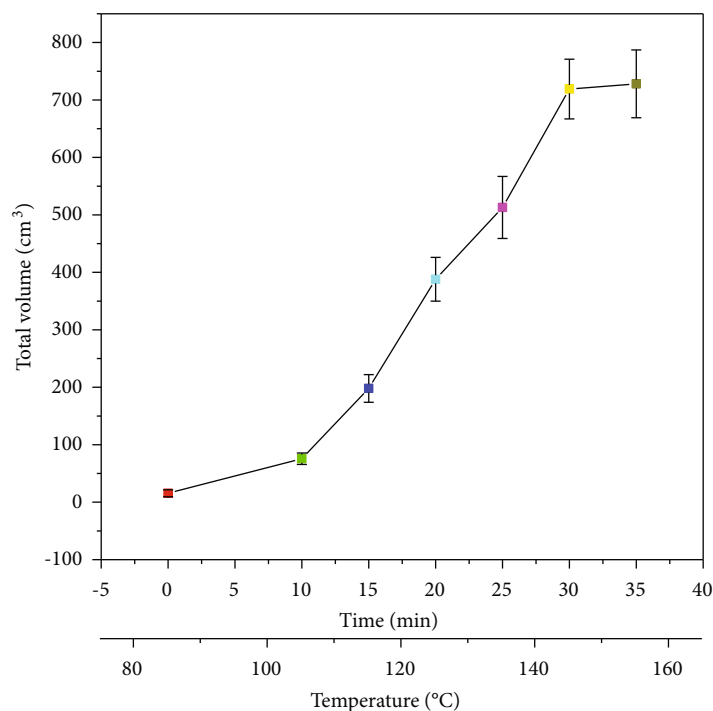


FIGURE 2: Volume expansion during foaming at various times (and temperature).

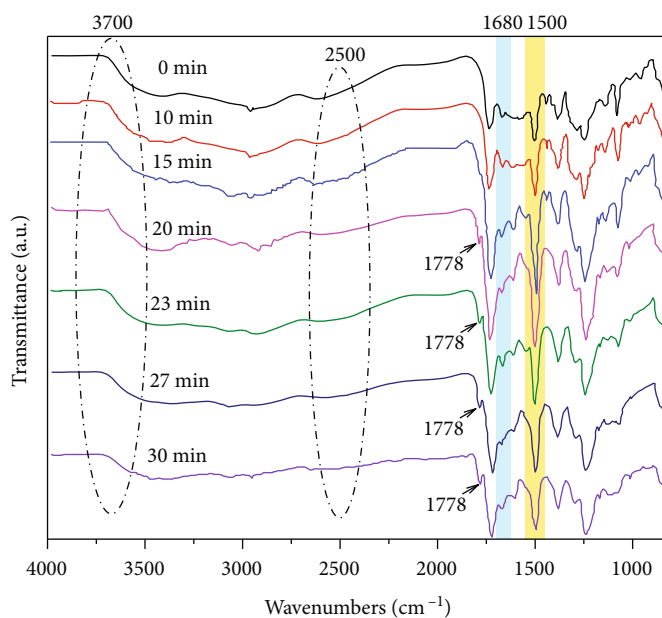


FIGURE 3: FTIR spectrum of PEAS foaming (150°C) at various times.

conceivable to speculate the possible distribution of aliphatic diamine in the BTDA/ODA-HMDA long chain polymer.

Theoretically, the amine groups on ODA should be more stable and relatively less reactive than the amine groups on HMDA. ODA has the π -electron stabilizing effect of the benzene ring to resonance with the lone pair electron on the amino group, while the latter does not. That being considered, the aliphatic amine will be kinetically favored over the ODA amine. On the other hand, in our designed relative molar ratio, highest content of HMDA was 20%, which

means that the ODA molecules will outnumber the HMDA molecules, which counterbalanced the above stated kinetic preference of HMDA. At low molar ratio, the aliphatic diamine should be inserted randomly on the polymer chain. On the other hand, at HMDA level higher than 25%, the polymers were gradually becoming more like elastomer and losing the required PI advantages. Similar observation was reported by Cristea et al. [17]. Therefore, the range of HMDA dosage studied in this study covered only from 0 to 20%.

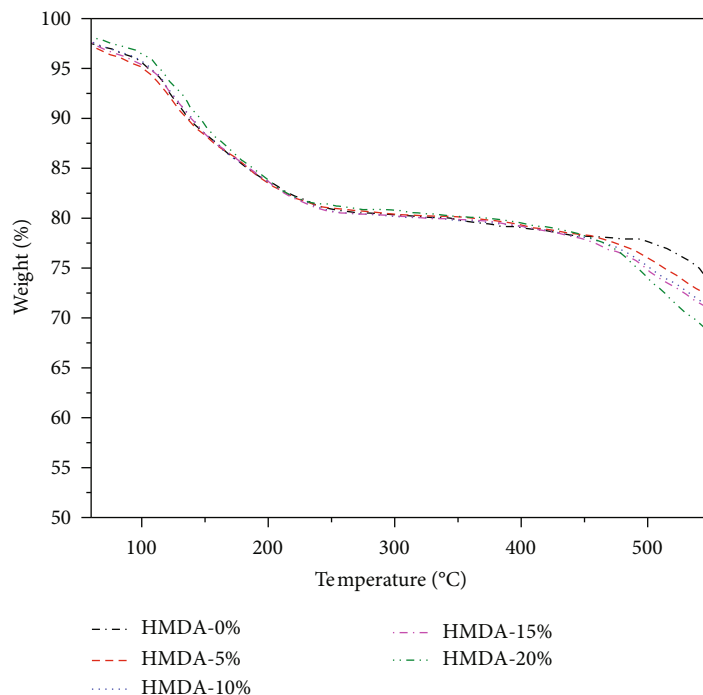


FIGURE 4: Weight loss (%) during forming and imidization with increasing temperature.

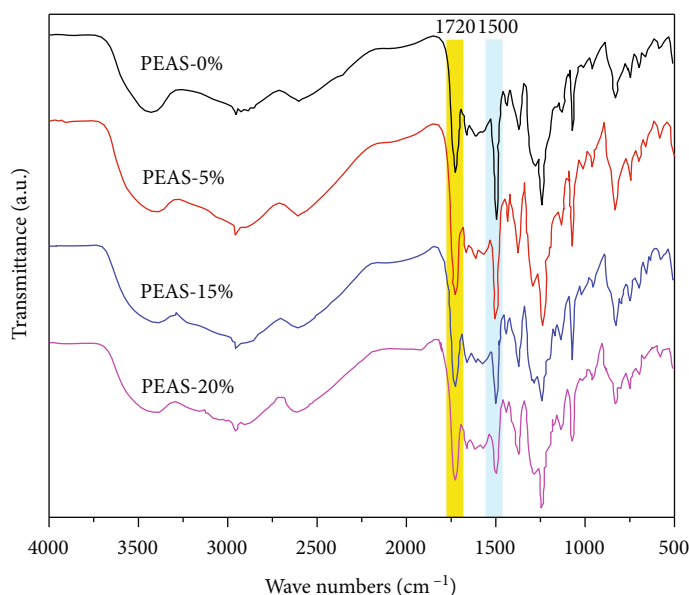


FIGURE 5: FTIR spectrum of PEAS with various HMDA contents.

This is consistent with the above analysis since increasing the more reactive HMDA could unavoidably affect the molecular homogeneity which might lead to uneven cell volume distribution. That being said, the aliphatic HMDA may have good chance of inserting in various places in the polymer chain. However, here we can merely present theoretical rationale until we studied the final product as will be discussed shortly.

For the foaming step, weighed PEAS precursor was evenly spread on the bottom of a stainless-steel box of 15 cm by 10 cm with depth of 15 cm with one side using

5 mm Pyrex glass for observation. A thin aluminum plate was placed on top of the foaming materials which will move in accordance with volume expansion. The box with sample was put into an oven in nitrogen. The temperature was raised to 150°C at a rate of 2.0°C/min and kept at 150°C for 1.5 h for imidization reaction and foaming to proceed. During imidization and foaming, as shown in Scheme 1, water (from condensation reaction) and methanol (from de-esterification) vaporized and expand, thus formed numerous cells (mostly closed cells at this time) which led to volume expansion of the whole loaf. The oven

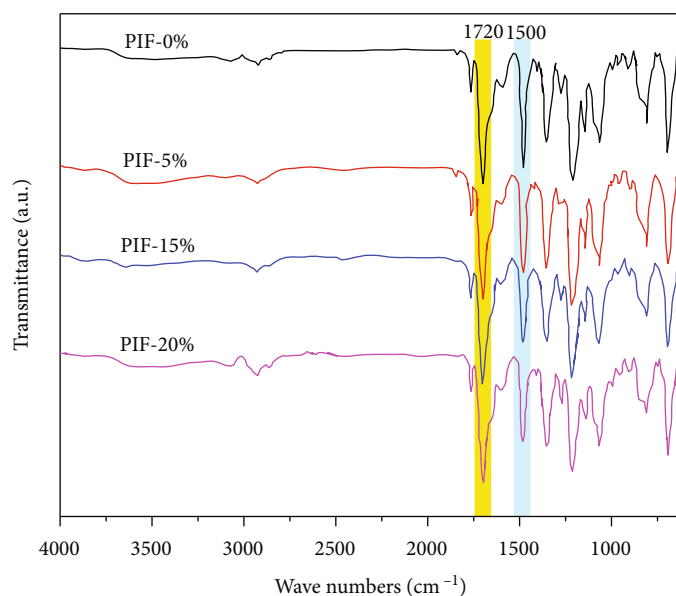


FIGURE 6: FTIR spectrum of PIFs with different HMDA contents.

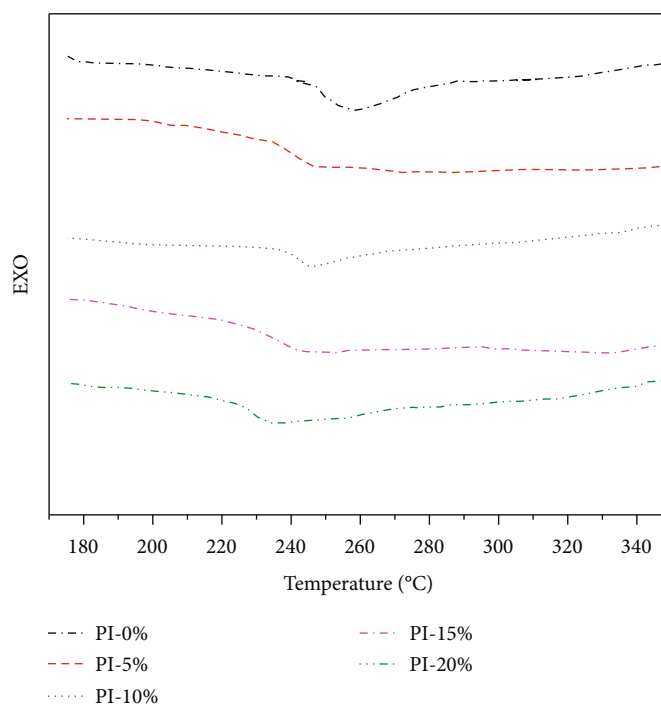


FIGURE 7: DSC curves of PIFs with different HMDA contents.

temperature was then raised to 300°C for the imidization and curing to go to completion for 1.5 h in nitrogen; this will be further discussed below.

In Table 1, for various designed HMDA content in PIFs, the molar ratio of BTDA to (ODA+HMDA) was fix at one, so that the total numbers of carbonyl function groups (of BTDA) and the amine groups (of ODA+HMDA) will be equal. Thus, the final PIFs with various compositions could be compared on grounds of the same total number of imide bonds.

3.2. Feature Changes of Functional Groups in the Reaction. FTIR spectrum provides important information about various function groups which may provide understanding the structure of the obtained polymer and explaining differences as resulted from various compositions. Figure 1 compare FTIR spectrum of the intermediate precursor PEAS (BTDA/ODA), PIF (BTDA/ODA), and PIF (BTDA/HMDA).

Featuring absorption peaks is the breathing of benzene ring at 1500 cm^{-1} , C-H stretching at 2800 & 2900 cm^{-1} , C=O of amide (1720 cm^{-1}), C=O of ester (1725 cm^{-1}),

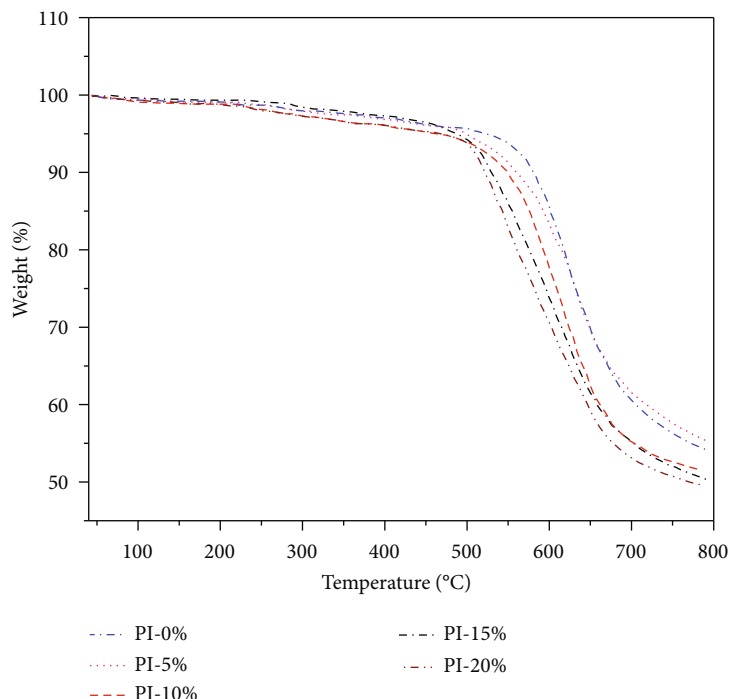


FIGURE 8: TGA curves of PIFs with various HMDA contents.

TABLE 2: Physical properties of PIFs with various HMDA contents.

Sample	T_g (°C)	T_d (10%) (°C)	10% compression stress (Kgf/cm ²)	Density (kg/m ³)
PIF-0	251	572	0.134	50
PIF-5	245	558	0.095	42
PIF-10	242	545	0.09	40
PIF-15	236	526	0.069	35
PIF-20	230	517	0.062	28

C=O of imide at 1778 cm^{-1} , and N-H stretching 3300 & 3400 cm^{-1} [57]. These will be discussed and compared below.

On FTIR spectrum of PEAS and PIFs, strong absorption peaks at 1500 cm^{-1} were observed. This characteristic peak was not seen on the HMDA spectra. The latter indicated that the lack of benzene ring (relatively BDTA or ODA do) [58], the HMDA has no absorption peak at 1500 cm^{-1} [59, 60]. For the PIF (BTDA+HMDA) spectrum in Figure 1, the C-H peaks at 2800 and 2900 cm^{-1} stood out comparing to the other two spectrum; the aliphatic C-H of HMDA are responsible for these absorption peaks.

Furthermore, the broad N-H stretching peaks (3300 & 3400 cm^{-1}) indicated the presence of unreacted amines in PEAS (BTDA/ODA). The absence of the broad N-H stretching peaks (3300 & 3400 cm^{-1}) on the PIF (BTDA/ODA) spectra is the evidence that all amine groups have participated in forming imide bonds. Again, in the PIF (BTDA/HMDA, no ODA) spectra, unreacted amines peaks (3300 & 3400 cm^{-1}), together with the observable small peak of imide C=O (1778 cm^{-1}), showed that the imidization reaction was not complete [61, 62].

3.3. Imidization and Foaming of PEAS. The foaming process is significantly affected by the melt viscosity of PEAS which form bubbles by evaporation of methanol and water and viscosity per se is an important operation parameter in the processing of PIF. Tian et al. [50] concluded that “the optimal foaming temperatures for PEAS powders ranged from 85 to 150°C ” and “thermal imidization process mainly takes place in the temperature between 150 and 250°C ”. Our observations are in line with their conclusion. This will be further discussed below.

In the process of preparing PIFs from PEAS, two types of distinct physical and chemical events were involved: foaming (cell expansion) and imidization. Foaming was caused by evaporation and expansion of methanol and water as generated from early stage of imidization. At this stage, imidization proceeded to only certain extent that the texture is still soft and flexible, which allowed the volume of the matrix responded promptly to gas (methanol and water) expansion, and rapid total volume increase was observed through the window on the oven.

Figure 2 depicted volume-time relationship for the initial 45 min. The volume increased rapidly between 10 and 25 min, but not significantly increased after 35 min, and

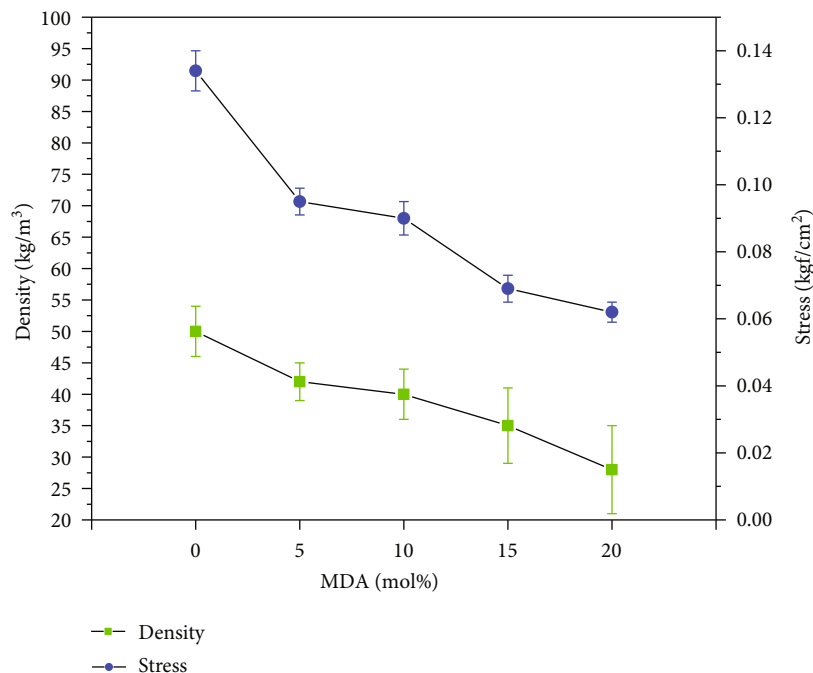


FIGURE 9: Density and 10% compression stress of PIFs with various HMDA contents.

remained virtually constant through 1.5 h, even after the oven temperature was raised to 300°C for another 1.5 h.

Figure 2 revealed that initially, temperature was low (increased at a rate of 2.0°C/min) resulting in low imidization rate, hence low gas generation rate, thereby low volume expansion (or low foaming rate). In the period between 10 and 25 min, the interior temperature should have reached 150°C, and the imidization rate increased along the course of heating. Meanwhile, the polymer matrix gradually loose its flexibility due to continued heating and imide bond formation. This should justify what was revealed in Figure 2 that no further volume increase observed after 35 min.

Figure 3 depicted the course (as recorded by FTIR spectrum) of the polymer function groups that went through during the foaming stage at 150°C as reported in the literature. Tian et al. [50] reported that the major thermal imidization took place in the range between 150 and 250°C. At the beginning (0 min), no imidization occurred yet; the imide C=O absorption peak at 1778 cm⁻¹ was not observed in the spectra. Meanwhile, the broad peak between 3700 and 2500 cm⁻¹ was due to the formed -NH₃⁺ and -COO⁻ salt.

As imidization time increased, the peak at 1778 cm⁻¹ became sharper, which indicates the formation of the imide C=O function group. On the other hand, the broad peak between 3700 and 2500 cm⁻¹ gradually flatten out through the progression of imidization.

Another feature worth noting in Figure 3 is that the diminishing absorption peaks of amide C=O at 1680 and 1550 cm⁻¹ (from 0 min to 30 min). Comparing the 30 min curve (in Figure 3) to the PIF curve in Figure 1, the above absorption peaks (in Figure 3) have not yet diminished to the relative intensity in Figure 1. This indicates imidization

has not yet come to completion. Meanwhile, the broad peaks between 3700 and 2500 cm⁻¹ are revealing the same information about imidization.

Information about the completion of the imidization process could be obtained by examining Figure 4, in which, the weight loss (due to methanol and water evaporation from open cells) sharply increased before 250°C. In the region of 250°C to 475°C, the weight remained virtually constant. However, the curve slightly sloped down in this region. This indicates that the imidization rate slowed down but not completely ended at 250°C. However, in this region the curve is rather flat, which indicates that there was only residual imidization taking place. Commonly in the preparation of PI, the step imidization processing temperature would stop at 300°C.

3.4. Featuring Function Groups of BTDA/ODA with and without HMDA. Thus far, we can think of at least three advantages of partially replacing ODA by HMDA: (1) HMDA costs much less than ODA, (2) aliphatic HMDA is more flexible that provides more design variable and processibility, and (3) high foaming ratio (possibly due to flexibility and elongation).

To verify the participation of the added HMDA in the imidization reaction as well as the foaming process, Figures 5 and 6 are presented for this purpose. Figure 5 compared FTIR spectrum of PEASs with different HMDA contents. The absorption peak at 1500 cm⁻¹ corresponds to benzene ring breathing of ODA [63] and was significantly sharp at 0% HMDA. When the amount of HMDA increased up to 20%, the 1500 cm⁻¹ peak gradually diminished. However, such contrasts could be made more profound by including another peak of fixed size as an internal standard.

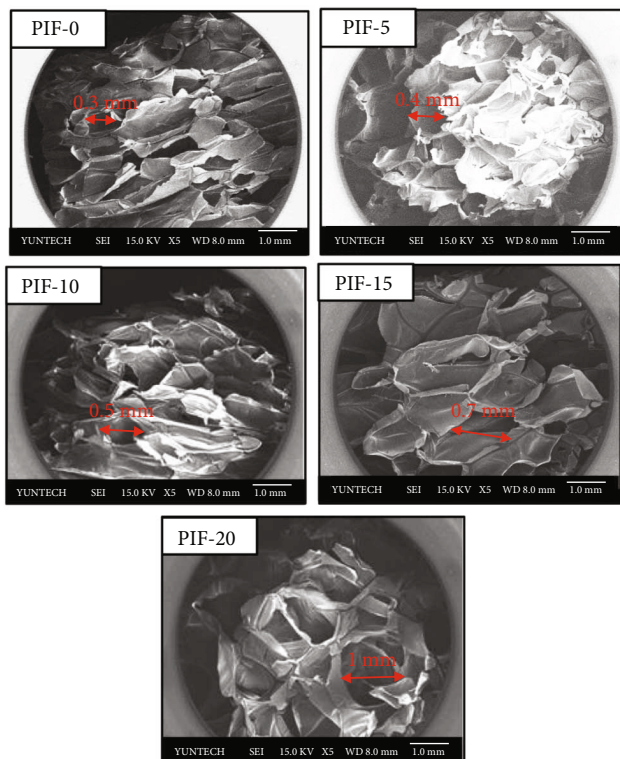


FIGURE 10: SEM images of cellular structure of PIFs with various HMDA contents.

In this case the imide C=O peak at 1720 cm^{-1} , the amount of which, as reflected on FTIR spectrum, is not affected by adding HMDA; hence, the peak intensity (of imide C=O) should not be affected either. Thus, if we compare the differences in heights of the 2 peaks, the above trend of decreased ODA aromatic with increased HMDA will be more obvious.

3.5. Thermal and Physical Properties

3.5.1. Glass Transition Temperature. Figure 7 compares the DSC curves of various HMDA content. Those fluctuations on the curve represent glass transition in polymer materials. The figure showed that all five tested samples have single T_g . This indicates that no microphase separation took place; otherwise, more than one T_g would have been observed. Figure 7 indicated that this did not happen at HMDA molar ratio below 20%. Single T_g of the tested specimen revealed that the resulting PIFs (with added HMDA) were homogeneous copolymers and that HMDA was randomly inserted in the aromatic chain. Cristea et al. [17] drew the same conclusion about this. On one hand, the inherent phenyl-phenyl ring attractions will lead to high intermolecular attraction, and pi-pi stacking of the aromatic ring enriched copolymer which resulted in high rigidity of the BTDA/ODA polyimide copolymer. On the other hand, inserting flexible aliphatic methylene group (of HMDA) would separate the phenyl rings apart and reduce the attraction force between them, hence will lead to reduction of rigidity. Reduced rigidity will, in turn, result in lower T_g of the polymer. Figure 7 showed

that T_g decreased with increasing HMDA content. T_g of PIFs synthesized in this study ranged from 230 to 251°C which is comparable to that reported by Cristea et al. [17].

3.5.2. Heat Decomposition Temperature. In this study, HMDA was introduced to partially replace ODA in PIFs for the purpose of down cost and to render flexibility to the copolymer. Figure 8 showed the results of thermal gravimetric analysis (TGA), and T_d (10%) temperatures are listed in Table 2. Similar to that of T_g , T_d (10%) decreased with increasing HMDA amount in the PIF copolymers. At HMDA content of 20%, T_d (10%) lowered (from 572°C) to 517°C. Cristea et al. [17] synthesized PI copolymers with various ratios of 4,4'-diaminodiphenylmethane (DDM) and HMDA and reported T_d of 455–490°C. Increased cost effectiveness at the price of losing some thermal durability may be worth the while in some applications. However, the original characteristic of PI as a good flame retardant would be affected. These results are comparable to that reported by Liu et al. [64] that the T_d (5%) values of their silver-coated PIFs were higher than 400°C.

3.5.3. Density and Rigidity. Density is an important design variable in the application of PIFs. The introduction of HMDA did not change the total number of imide bonds; rather, the molar mass (HMDA 116 g/mol vs. ODA 200 g/mol) was changed, which is the first reason that resulted in changed density. Compared to ODA with benzene ring structure, the aliphatic HMDA is more flexible and will allow more room for volume expansion during foaming, which is the second reason for density variation. Therefore, density dropped (from 50 to 28 kg/m³) with increased amount of HMDA added, as shown in Table 2 and Figure 9. Liu et al. [64] synthesized novel PIFs (using two solution method with pyromellitic dianhydride) with an apparent density of ca 14.5 kg/m³. Yan et al. [37] obtained, by using vermiculite dispersed in isocyanate, a flexible polyimide composite foam with a density of 10 kg/m³. The densities of PIFs in this study are in the lower range of TEEK foams [65] (8 to 320 kg/m³) as reported by Yang et al. [6]. Low density could be advantageous when thermal durability and rigidity are not seriously concerned. In a similar manner, added HMDA will lead to decreased rigidity. Compression stress at 10% deformation was chosen as the criteria for comparison; results are shown in Table 2 and Figure 9. As can be seen from test results, the 10% compression stress decreased with increasing HMDA content.

3.5.4. Foam Cells. In the reaction of forming one imide bond, one molecule of water and one molecule of methanol were released (Scheme 1). At the reaction temperature of 150°C, water and methanol vaporized and expanded rapidly, thus foaming took place due to generated water and methanol vapors which formed cells in the PI matrix (which is elastic before certain stage of curing). During imidization process, the viscous fluid of PEAS matrix gradually lost its fluidity and solidified and then gradually increased rigidity. These cells should stay as hollow chambers throughout the completion of the imidization and foaming. For the purpose of

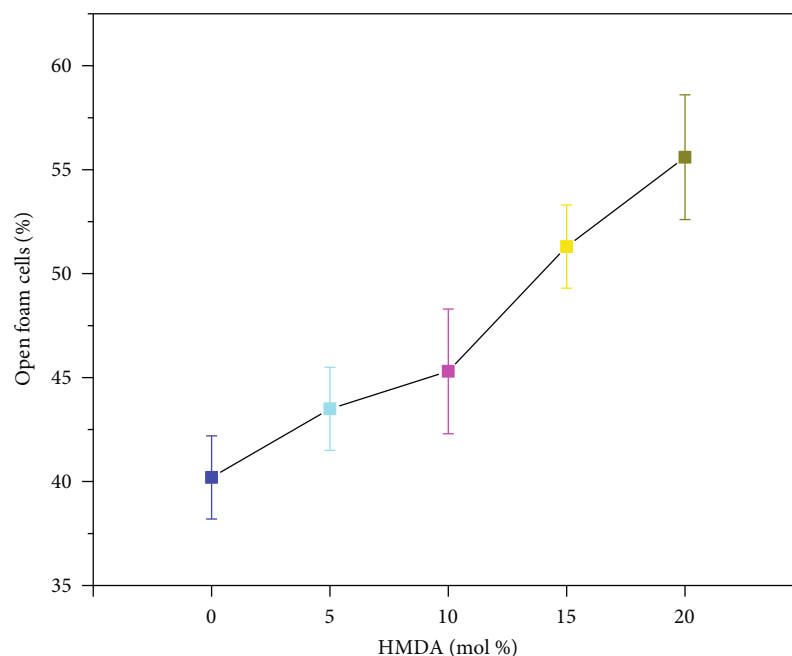


FIGURE 11: % open cells of PIFs with various HMDA contents.

further completing the imidization reaction, the temperature was further increased to 300°C. During this stage, increased temperature will further increase the vapor pressures of water and methanol. If the pressure of water and methanol vapor exceeds the restraining force of surrounding PI matrix, some of the foam cells would break and formed “open cells”. Otherwise, most of the foam cells would have been closed cells (at least initially).

As stated above, introducing flexible aliphatic diamines provides additional flexibility to the PI copolymer. This is important in determining, for fixed initial amount of starting materials, the final volume of the foam, size of the foam cells, and number of open cells. In effect, flexibility increases expansibility and thus the cell size. Figure 10 compared the SEM of PIF slice, which verified such trend. As the cell size increased to some extent, the wall of foam cells became thinner accordingly. Foam cells with thin wall are easier to break. Figure 11 showed that the number of open cells increased with increasing the HMDA content. The increase of about 17% open cell was observed at 20% HMDA. The above stated results showed that pretreatment temperature and foaming temperature are consistent with that reported by Li et al. [42].

Foam cell is an important physical barrier for heat transfer. From this perspective, PIFs with more foam cells (whether in numbers, volumes, or both) would be better thermal insulators. Further, closed cells with near vacuum interior, due to later condensation of water and methanol, would be a better insulator than open cells. Still, the latter would be a better insulator than the solid polymer matrix. Figure 9 showed that for the same amount of starting material, PIF with 20% HMDA has a specific volume (m^3/kg , reciprocal of density) of 80% higher than that without HMDA. This means that PIF with 20% HMDA has a foam cell volume (close and open cell) that was 80% higher than

that without HMDA. Since more or larger cell volume should create more barrier for heat transfer (heat transfer rate for gases is much less than for solids), taking into account the 17% increase of open cell, PIF with 20% HMDA may be a better thermal insulator than that without HMDA. Although no quantitative data of thermal insulation was presented in this report, it is fair to say at this point, that for lowered manufacturing cost and better thermal insulation, the tradeoff of compromised rigidity may be worthy.

Above 20% HMDA, the foaming cell of PIFs was less evenly distributed, and cell size was less uniform. When we further increased the HMDA content, the copolymer gradually lost the advantages of PI and became more and more like an elastomer, as reported in a similar research by Cristea et al. [17].

4. Conclusions

This research proposed a new PIF formulation by inserting a flexible aliphatic diamine (HMDA) to the main backbone of PI. The primary motive was to lower the cost of PIF production. Although at 20% substitution, the cost difference was not overwhelmingly large (about 75% price difference between ODA and HMDA); the flexible HMDA conferred various desirable properties to the foam. FTIR studies provided evidences that instead of physical mixing, HMDAs participated in the PIF forming reactions and were chemically bonded with the aromatic dianhydride moieties. Added flexibility of HMDA increased the volume of the foam per unit mass of starting materials, which resulted in decreased density of the foam. Consequently, the rigidity and thermal durability were affected. T_d (10%) dropped from 572°C (without HMDA) to 517°C (20% HMDA), and the latter is still in the 500°C range which is higher than the requirement of a common high-temperature thermal insulator. The range

of added amount of HMDA (0 to 20%) can be considered as a new variable in designing novel PIFs to meet various demands. Processing details may affect the final outcome. For example, Hou et al. [65] reported that the degree of foaming is significantly affected by processing heating rate, and hold temperature was not investigated in this study which will be an interesting area to be explored. In summary, this work provided a feasible approach for preparing lightweight and mechanically flexible PIFs which demonstrate potential high-temperature thermal insulation applications in various industries.

Data Availability

The data used to support the findings of this study are included in the article. Further data or information is available from the corresponding author upon request.

Conflicts of Interest

The authors declare that they have no conflicts of interest.

Acknowledgments

This work is supported by Industrial Technology Research Institute (ITRI) and National Yang Ming Chiao Tung University.

References

- [1] S. Ikeda, H. Yanagimoto, K. Akamatsu, and H. Nawafune, "Copper/polyimide heterojunctions: controlling interfacial structures through an additive-based, all-wet chemical process using ion-doped precursors," *Advanced Functional Materials*, vol. 17, no. 6, pp. 889–897, 2007.
- [2] P. Ma, C. Dai, H. Wang et al., "A review on high temperature resistant polyimide films: heterocyclic structures and nanocomposites," *Composites Communications*, vol. 16, pp. 84–93, 2019.
- [3] N. Ohta, Y. Nishi, T. Morishita, T. Tojo, and M. Inagaki, "Preparation of microporous carbon films from fluorinated aromatic polyimides," *Carbon*, vol. 46, no. 10, pp. 1350–1357, 2008.
- [4] I. Gouzman, E. Grossman, R. Verker, N. Atar, A. Bolker, and N. Eliaz, "Advances in polyimide-based materials for space applications," *Advanced Materials*, vol. 31, no. 18, pp. 1807738–1807755, 2019.
- [5] Y. H. Zhang, S. Y. Fu, R. K.-Y. Li et al., "Investigation of polyimide-mica hybrid films for cryogenic applications," *Composites Science and Technology*, vol. 65, no. 11–12, pp. 1743–1748, 2005.
- [6] S. Y. Yang, H. X. Yang, and A. J. Hu, "Super engineering plastics and forms," *Advanced Polyimide Materials: Synthesis, Characterization, and Applications*, Elsevier, pp. 173–193, 2018.
- [7] J. W. Park, M. Lee, M.-H. Lee et al., "Synthesis and characterization of soluble alternating aromatic copolyimides," *Macromolecules*, vol. 27, no. 13, pp. 3459–3463, 1994.
- [8] M. G. Dhara and S. Banerjee, "Fluorinated high-performance polymers: poly(arylene ether)s and aromatic polyimides containing trifluoromethyl groups," *Progress in Polymer Science*, vol. 35, no. 8, pp. 1022–1077, 2010.
- [9] Q. Xia, J. Liu, J. Dong et al., "Synthesis and characterization of high-performance polyimides based on 6,4'-diamino-2-phenylbenzimidazole," *Journal of Applied Polymer Science*, vol. 126, pp. 145–151, 2013.
- [10] M. Ree, "High performance polyimides for applications in microelectronics and flat panel displays," *Macromolecular Research*, vol. 14, no. 1, pp. 1–33, 2006.
- [11] A. E. Eichstadt, T. C. Ward, M. D. Bagwell, I. V. Farr, D. L. Dunson, and J. E. McGrath, "Synthesis and characterization of amorphous partially aliphatic polyimide copolymers based on bisphenol-A dianhydride," *Macromolecules*, vol. 35, no. 20, pp. 7561–7568, 2002.
- [12] Y. Xiao, B. T. Low, S. S. Hosseini, T. S. Chung, and D. R. Paul, "The strategies of molecular architecture and modification of polyimide-based membranes for CO₂ removal from natural gas—a review," *Progress in Polymer Science*, vol. 34, no. 6, pp. 561–580, 2009.
- [13] Y. Ha, Y. Kim, and C. S. Ha, "Nanoscale blending of aliphatic and aromatic polyimides: a clue for forming semi-molecular composites and in-situ generation of copolyimide fractions," *Polymer Bulletin*, vol. 59, no. 6, pp. 833–845, 2008.
- [14] S. Chisca, V. E. Musteata, I. Stoica, I. Sava, and M. Bruma, "Effect of the chemical structure of aromatic-cycloaliphatic copolyimide films on their surface morphology, relaxation behavior and dielectric properties," *Journal of Polymer Research*, vol. 20, no. 3, pp. 1–11, 2013.
- [15] H. Choi, B. Sohn, and J. H. Chang, "Synthesis and characterization of transparent copolyimide films containing CF₃ groups: comparison with copolyimide nanocomposites," *Applied Clay Science*, vol. 48, no. 1–2, pp. 117–126, 2010.
- [16] A. E. Eichstadt, T. C. Ward, M. D. Bagwell, I. V. Farr, D. L. Dunson, and J. E. McGrath, "Structure-property relationships for a series of amorphous partially aliphatic polyimides," *Journal of Polymer Science Part B: Polymer Physics*, vol. 40, no. 14, pp. 1503–1512, 2002.
- [17] M. Cristea, D. Ionita, C. Hulubei, D. Timpu, D. Popovici, and B. C. Simionescu, "Chain packing versus chain mobility in semialiphatic BTDA-based copolyimides," *Polymer*, vol. 52, no. 8, pp. 1820–1828, 2011.
- [18] N. Asano, M. Aoki, S. Suzuki, K. Miyatake, H. Uchida, and M. Watanabe, "Aliphatic/aromatic polyimide ionomers as a proton conductive membrane for fuel cell applications," *Journal of the American Chemical Society*, vol. 128, no. 5, pp. 1762–1769, 2006.
- [19] C. D. Varganici, D. Rosu, C. Barbu-Mic et al., "On the thermal stability of some aromatic-aliphatic polyimides," *Polyimides Journal of Analytical and Applied Pyrolysis*, vol. 113, pp. 390–401, 2015.
- [20] T. Ogura and M. Ueda, "Facile synthesis of semiaromatic poly(amic acid)s from trans-1,4-cyclohexanediamine and aromatic tetracarboxylic dianhydrides," *Macromolecules*, vol. 40, no. 10, pp. 3527–3529, 2007.
- [21] J. E. McGrath, D. L. Dunson, S. J. Mechem, and J. L. Hedrick, "Synthesis and characterization of segmented polyimide-polyorganosiloxane copolymers," *Progress in Polyimide Chemistry I*, vol. 1, pp. 61–105, 1999.
- [22] W. C. Liaw, J. Chang-Chian, H. Kang, Y. L. Cheng, and L. W. Fu, "A straightforward synthesis and characterization of a new poly(imide siloxane)-based thermoplastic elastomer," *Polymer Journal*, vol. 40, no. 2, pp. 116–125, 2008.

- [23] W. C. Liaw, Y. L. Cheng, Y. S. Liao, C. S. Chen, and S.-M. Lai, "Complementary functionality of SiO₂ and TiO₂ in polyimide/silica-titania ternary hybrid nanocomposites," *Polymer Journal*, vol. 43, no. 3, pp. 249–257, 2011.
- [24] A. P. Nowak, A. F. Gross, K. Drummey et al., "Visually and infrared transparent poly(oxalamide) films with mechanical toughness," *ACS Applied Polymer Materials*, vol. 4, no. 7, pp. 5027–5034, 2022.
- [25] S. H. Park, A. Alammari, Z. Fulop, B. A. Pulido, S. P. Nunes, and G. Szekely, "Hydrophobic thin film composite nanofiltration membranes derived solely from sustainable sources," *Green Chemistry*, vol. 23, no. 3, pp. 1175–1184, 2021.
- [26] C. Yang, F. Topuz, S. H. Park, and G. Szekely, "Biobased thin-film composite membranes comprising priamine–genipin selective layer on nanofibrous biodegradable polylactic acid support for oil and solvent-resistant nanofiltration," *Green Chemistry*, vol. 24, no. 13, pp. 5291–5303, 2022.
- [27] W. R. Hendrix, *DuPont, U.S. Patent 3*, 1966.
- [28] N. Teo, Z. P. Gu, and S. C. Jana, "Polyimide-based aerogel foams, via emulsion-templating," *Polymer*, vol. 157, pp. 95–102, 2018.
- [29] Y. Y. Wang, Z. H. Zhou, C. G. Zhou et al., "Lightweight and robust carbon nanotube/polyimide foam for efficient and heat-resistant electromagnetic interference shielding and microwave absorption," *ACS Applied Materials & Interfaces*, vol. 12, no. 7, pp. 8704–8712, 2020.
- [30] L. Ni, Y. Luo, X. Peng, S. Zhou, H. Zou, and M. Liang, "Investigation of the properties and structure of semi-rigid closed-cellular polyimide foams with different diamine structures," *Polymer*, vol. 229, pp. 123957–123959, 2021.
- [31] Y. Shi, A. Hu, Z. Wang, K. Li, and S. Yang, "Closed-Cell Rigid Polyimide Foams for High-Temperature Applications: The Effect of Structure on Combined Properties," *Polymers*, vol. 13, no. 24, p. 4434, 2021.
- [32] H. Liu, X. Chen, Y. Zheng et al., "Lightweight, superelastic, and hydrophobic polyimide nanofiber /MXene composite aerogel for wearable piezoresistive sensor and oil/water separation applications," *Advanced Functional Materials*, vol. 31, no. 13, pp. 2008006–2008017, 2021.
- [33] J. C. Johnston, M. A. B. Meador, and W. B. Alston, "A mechanistic study of polyimide formation from diester-diacids," *Journal of Polymer Science Part A: Polymer Chemistry*, vol. 25, no. 8, pp. 2175–2183, 1987.
- [34] M. K. Ghosh and K. L. Mittal, *Polyimides: Fundamentals and Applications*, Marcel Dekker, New York, 1996, <https://searchworks.stanford.edu/view/3378363>.
- [35] E. S. Weiser, T. F. Johnson, T. L. St Clair, Y. Echigo, H. Kaneshiro, and B. W. Grimsley, "Polyimide foams for aerospace vehicles," *High Performance Polymers*, vol. 12, no. 1, pp. 1–12, 2000.
- [36] J. Li, G. Zhang, J. Li, L. Zhou, Z. Jing, and Z. Ma, "Preparation and properties of polyimide/chopped carbon fiber composite foams," *Polymers for Advanced Technologies*, vol. 28, no. 1, pp. 28–34, 2017.
- [37] L. Yan, L. Fu, Y. Chen, H. Tian, A. Xiang, and A. V. Rajulu, "Improved thermal stability and flame resistance of flexible polyimide foams by vermiculite reinforcement," *Journal of Applied Polymer Science*, vol. 134, no. 20, pp. 44828–44835, 2017.
- [38] H. Tian, Y. Yao, S. Ma, J. Wu, and A. Xiang, "Enhanced thermal stability and flame resistance of polyurethane-imide foams by adding silicon carbide," *Advances in Polymer Technology*, vol. 37, no. 7, 2477 pages, 2018.
- [39] L. Zhou, Y. Cai, D. Shen et al., "Anti-oxidation polyimide-based hybrid foams assembled with bilayer coatings for efficient electromagnetic interference shielding," *Chemical Engineering Journal*, vol. 451, no. 3, pp. 138808–138818, 2023.
- [40] M. B. Meador, E. J. Malow, R. Silva et al., "Mechanically strong, flexible polyimide aerogels cross-linked with aromatic triamine," *ACS Applied Materials & Interfaces*, vol. 4, no. 2, pp. 536–544, 2012.
- [41] H. J. Chu, B. K. Zhu, and Y. Y. Xu, "Polyimide foams with ultralow dielectric constants," *Journal of Applied Polymer Science*, vol. 102, no. 2, pp. 1734–1740, 2006.
- [42] J. Li, N. Yu, Z. Jing, X. He, X. Shi, and G. Zhang, "Fabrication of rigid polyimide foams via thermal foaming of nadimide-end-capped polyester-amine precursor," *Polymer Bulletin*, vol. 77, no. 11, pp. 5899–5912, 2020.
- [43] L. Wang, A. Hu, L. Fan, and S. Yang, "Structures and properties of closed-cell polyimide rigid foams," *Journal of Applied Polymer Science*, vol. 130, no. 5, pp. 3282–3291, 2013.
- [44] J. Li, G. Zhang, Y. Yao, Z. Jing, L. Zhou, and Z. Ma, "Synthesis and properties of polyimide foams containing benzimidazole units," *RSC Advances*, vol. 6, no. 65, pp. 60094–60100, 2016.
- [45] H. Zhang, X. Fan, W. Chen et al., "A simple and green strategy for preparing flexible thermoplastic polyimide foams with exceptional mechanical, thermal-insulating properties, and temperature resistance for high-temperature lightweight composite sandwich structures," *Composites Part B: Engineering*, vol. 228, pp. 109405–109408, 2022.
- [46] X. Y. Liu, M. S. Zhan, K. Wang, Y. Li, and Y. F. Bai, "Preparation and performance of a novel polyimide foam," *Polymers for Advanced Technologies*, vol. 23, no. 3, pp. 677–685, 2012.
- [47] G. Sun, L. Liu, J. Wang, H. Wang, Z. Xie, and S. Han, "Enhanced polyimide proportion effects on fire behavior of isocyanate-based polyimide foams by refilled aromatic dianhydride method," *Polymer Degradation and Stability*, vol. 110, pp. 1–12, 2014.
- [48] J. W. Li, N. Yu, Y. Q. Ding et al., "Fabrication of rigid polyimide foams with overall enhancement of thermal and mechanical properties," *Journal of Cellular Plastics*, vol. 57, no. 5, pp. 717–731, 2021.
- [49] J. W. Li, Y. Q. Ding, N. Yu et al., "Lightweight and stiff carbon foams derived from rigid thermosetting polyimide foam with superior electromagnetic interference shielding performance," *Carbon*, vol. 158, pp. 45–54, 2020.
- [50] H. F. Tian, Y. Y. Yao, S. B. Ma, L. W. Fu, A. M. Xiang, and A. V. Rajulu, "Improved mechanical, thermal and flame resistant properties of flexible isocyanate-based polyimide foams by graphite incorporation," *High Performance Polymers*, vol. 30, no. 9, pp. 1130–1138, 2018.
- [51] M. Yang, C. Zhang, Q. Lv et al., "Rational design of novel efficient palladium electrode embellished 3D hierarchical graphene/polyimide foam for hydrogen peroxide electroreduction," *ACS Applied Materials & Interfaces*, vol. 12, no. 1, pp. 934–944, 2020.
- [52] Y. Luo, L. Ni, L. Yan, H. Zou, S. Zhou, and M. Liang, "Structure to properties relations of polyimide foams derived from various dianhydride components," *Industrial & Engineering Chemistry Research*, vol. 60, no. 26, pp. 9489–9499, 2021.
- [53] L. Ni, Y. Luo, C. Qiu et al., "Mechanically flexible polyimide foams with different chain structures for high temperature

- thermal insulation purposes,” *Materials Today Physics*, vol. 26, pp. 100720–100728, 2022.
- [54] L. Y. Pan, M. S. Zhan, and K. Wang, “Preparation and characterization of high-temperature resistance polyimide foams,” *Polymer Engineering & Science*, vol. 50, no. 6, pp. 1261–1267, 2010.
- [55] K. Qi, G. Zhang, S. Li, L. Liu, and Z. Hel, “Preparation and properties of high performance polyimide foam,” *Advanced Materials Research*, vol. 221, pp. 66–71, 2011.
- [56] W. Leilei, H. Aijun, F. Lin, and Y. Shiyong, “Structures and properties of closed-cell polyimide rigid foams,” *Journal of Applied Polymer Science*, vol. 130, no. 5, pp. 3282–3291, 2013.
- [57] L. Junpeng, Z. Qinghua, X. Qingming, D. Jie, and X. Qian, “Synthesis, characterization and properties of polyimides derived from a symmetrical diamine containing bis-benzimidazole rings,” *Polymer Degradation and Stability*, vol. 97, no. 6, pp. 987–994, 2012.
- [58] Spectral Database for Organic Compounds SDBS-ODA https://sdb.sdb.aist.go.jp/sdbs/cgi-bin/direct_frame_disp.cgi?sdbno=10695&spectrum_type=IR&fname=NIDA7712.
- [59] Spectral Database for Organic Compounds SDBS-BTD https://sdb.sdb.aist.go.jp/sdbs/cgi-bin/direct_frame_disp.cgi?sdbno=7780&spectrum_type=IR&fname=NIDA13437.
- [60] S. Rimdusit and C. Jubsilp, “Properties enhancement obtained in anhydride-modified polybenzoxazines: effects of ester functional group on polybenzoxazine network,” *Advanced and Emerging Polybenzoxazine Science and Technology*, Elsevier, pp. 147–170, 2017.
- [61] C. Huang, J. Li, G. Zhang, R. Sun, and C. P. Wong, “Development of low temperature curing polyimides with quinoline,” in *20th International Conference on Electronic Packaging Technology (ICEPT)*, pp. 1–4, 2019, <https://ieeexplore.ieee.org/document/9080920>.
- [62] Y. Xu, A. Zhao, X. Wang, H. Xue, and F. Liu, “Influence of curing accelerators on the imidization of polyamic acids and properties of polyimide films,” *Journal of Wuhan University of Technology-Mater. Sci. Ed.*, vol. 31, no. 5, pp. 1137–1143, 2016.
- [63] C. C. Yang, K. H. Hsieh, and W. C. Chen, “A new interpretation of the kinetic model for the imidization reaction of PMDA-ODA and BPDA-PDA poly(amic acids),” *Polyimides and Other High Temperature Polymers*, vol. 2, pp. 37–45, 2003.
- [64] X. Y. Liu, M. S. Zhan, and K. Wang, “Preparation and characterization of electromagnetic interference shielding polyimide foam,” *Journal of Applied Polymer Science*, vol. 127, no. 5, pp. 4129–4137, 2012.
- [65] T. H. Hou, E. S. Weiser, E. J. Siochi, and T. L. St Clair, “Processing characteristics of TEEK polyimide foam,” *High Performance Polymers*, vol. 16, no. 4, pp. 487–504, 2004.